First-principles study of 1,4-butanedithiol molecules and radicals adsorbed on unreconstructed Au(111) and Au(100)

A. Franke* and E. Pehlke

Institut für Theoretische Physik und Astrophysik, Christian-Albrechts-Universität zu Kiel, 24098 Kiel, Germany

(Received 15 September 2009; revised manuscript received 5 January 2010; published 8 February 2010)

Ongoing experimental research effort is devoted to further the understanding of the adsorption of dithiol molecules on gold surfaces with promising technological applications. To elucidate the subject from a theoretical perspective, we study the submonolayer adsorption of 1,4-butanedithiol molecules and radicals on the unreconstructed Au(111) and Au(100) surfaces using density-functional theory. From the calculated local energy minima the lowest-energy configurations are selected. The alkane chains are roughly parallel to the surface, such that two sulfur-gold adsorbate-substrate bonds can form. On the unreconstructed Au(100) surface dissociation of butanedithiol molecules into H_2 in the gas phase and butanedithiol radicals chemisorbed on the surface is energetically preferred. The two sulfur atoms of the radical adopt hollow-bridge-like positions. On the unreconstructed Au(111) surface the S-H bonds are predicted to be cleaved due to entropic effects. In the ground-state configuration the two sulfur atoms of the butanedithiol radical adopt an fcc hollow and an fcc hollow-bridge position on the surface. Hence, we expect butanedithiol radicals to be the prevailing adsorbed species on both investigated gold surfaces. STM-images of the ground-state configuration of butanedithiol radicals chemisorbed on Au(111) have been simulated within the Tersoff-Hamann model. They show elongated bright features above the location of the alkane chain. The long axis is slightly tilted with respect to the $\langle 1\bar{1}0\rangle$ directions. Finally, a semiempirical approach has been evaluated to investigate the effect of van der Waals interactions to the binding energies calculated within GGA-DFT.

DOI: 10.1103/PhysRevB.81.075409 PACS number(s): 68.43.Bc, 68.43.Fg, 82.65.+r, 64.75.Yz

I. INTRODUCTION

The pursuit of miniaturization in fields such as microelectronics and biosensor technology has lead to an increased interest in functionalized metal or semiconductor surfaces.[1] The synthesis of organic molecular assemblies at the surface is a widely utilized method to achieve such a functionalization.[1,2] Organic molecules offer the prospect of tailor-made functionalizations by choosing specific end groups of the adsorbates.[2] Prominent examples include the fabrication of switchable molecular assemblies on the surface.[3–11]

Among the most widely studied systems are self-assembled monolayers (SAMs) of sulfur bonded thiol molecules at Au surfaces. In particular, SAMs of alkanedithiols in which one of the thiol groups is adsorbed on the surface while the other is pointing away from the surface, are considered promising building blocks of future nanodevices.[12–15] The thiol group at the top of the alkane chain offers the possibility to serve, e.g., as an anchor for cadmium-selenide nanocrystals in single electron transistors (Ref. 12), metal contacts in molecular dithiol junctions (Refs. 13, 14, and 16–20), metal and metal-oxide clusters (Ref. 21–28), as well as metallic thin films (Refs. 29 and 30). From a fundamental point of view, alkanedithiols are regarded as an important model system for organic sulfur bonded molecules.[2,15]

In recent years intense experimental research effort is devoted to the adsorption of different dithiol molecules on the Au(111) surface under ultra high vacuum (UHV), ambient as well as electrochemical (EC) conditions.[19,31–41] However, the details of metastable adsorption phases and equilibrium structures remains controversial. The existence of two thiol groups within the molecule raises the question whether dithiol molecules bind via one (upright configuration) or two (lying-down configuration) Au-S bonds to the surface. In case of the most common deposition methods either from the gas phase or from solution both upright (Refs. 19, 32, 36, 37, and 42) and lying-down configurations (Refs. 19, 32–37, and 43) were observed. It was reported that dithiol molecules can polymerize upon adsorption on the surface forming multilayers of molecules connected through S-S bonds.[38–41,44,45] Furthermore, butanedithiol adsorbates have been observed in video scanning tunneling microscopy experiments at low and saturation coverages under EC conditions on the unreconstructed Au(111) surface.[46]

The adsorption configurations of upright and lying-down alkanedithiol molecules at Au surfaces thus call for detailed density-functional studies. The focus of our present work is to compare the adsorption of 1,4-butanedithiol molecules [BDT: $HS\text{-}(CH_2)_4\text{-}SH$] and BDT radicals [BDTR: $\cdot S\text{-}(CH_2)_4\text{-}S\cdot$] at submonolayer coverages on the unreconstructed Au(111) and Au(100) surfaces. Polymerization of BDT molecules or radicals is beyond the scope of the present work. Adsorption properties on unreconstructed Au surfaces are relevant in case of EC conditions, where a potential-induced lifting of the Au(111) and Au(100) surface reconstructions can be achieved.[47,48]

The BDT and BDTR adsorption configurations on Au(111) and Au(100) surfaces reported below currently serve as a starting point for the investigation of the BDT and BDTR diffusion dynamics. In our view, this knowledge is indispensable to a deeper understanding of self assembly at Au surfaces and the diffusion of molecular adsorbates with one or two sulfur bonds to the Au surface.[49–63]

The present paper is organized in the following manner. Section II summarizes the calculational details of our work.

In Secs. III A 1 and III A 2 we present adsorption configurations of the BDT molecule and radical on the unreconstructed Au(111) surface. Adsorption of BDT molecules and radicals on the Au(100) surface is discussed in Secs. III B 1 and III B 2. In order to assess the importance of surface defects, we consider the adsorption of BDT radicals in the presence of adatoms and vacancies on the Au(111) surface in Sec. III A 3 and on the Au(100) surface in Sec. III B 3. Sections III A 4 and III B 3 are devoted to the question whether BDT adsorbs as molecules or radicals on the Au(111) and Au(100) surface. Simulated scanning tunneling microscopy (STM) images are reported in Sec. III A 5.

II. CALCULATIONAL METHOD

Relaxed adsorption configurations for BDT and BDTR on the unreconstructed Au(111) and Au(100) surfaces have been calculated within density-functional theory using slab geometries. First we choose a set of initial configurations, which are relaxed to local chemisorption energy minima. The initial configurations differ by the positions of the two sulfur atoms with respect to the underlying substrate and the conformation of the adsorbed BDT molecule or radical. To reduce computational costs, the convergence criteria have been alleviated for this survey. We select the lowest-energy structures from this survey and recalculate the total energies for frozen-in atomic coordinates at increased values for plane-wave cutoff energy, number of **k** points, and number of bulklike Au layers in the slab. We have verified that the ordering with respect to chemisorption energy is not affected (see Appendix C).

The total energy of the electronic ground state has been calculated using the Vienna *ab initio* simulation program (VASP) (Refs. 64–67) developed at the Institut für Materialphysik of the Universität Wien which is based on density-functional theory. The generalized gradient approximation (GGA) by Perdew and Wang (PW91) (Ref. 68) is applied to the exchange-correlation functional and the electron-ion interaction is treated within the framework of Blöchl's projector augmented wave method (PAW).[69,70] The potentials for VASP from the database are used.[70]

The periodically repeated gold slabs are separated by a vacuum region of at least 12 Å. Asymmetric slabs have been chosen, i.e., the adsorbate binds to a single side of the slab only. A dipole correction is applied in order to account for the work function difference between the opposite surfaces of the slab.

The initial survey has been carried through with slabs comprising 4 layers of gold and a (4×3) or (4×4) surface unit cell. The Kohn-Sham wave functions are expanded in a plane-wave basis set with a cutoff energy of 250 eV. Plane waves up to an energy of 750 eV are used to represent the augmentation charges. The integrals over the Brillouin zone are approximated by sums over special **k** points (Ref. 71) using meshes consisting of 12 and 9 **k** points in the complete first Brillouin zone of the (4×3) and (4×4) surface unit cell, respectively. The **k**-point meshes are equivalent.

The gold atoms in the outermost three layers on the adsorbate side of the slab as well as all adsorbate atoms are relaxed without constraints until the residual force per atom is smaller than 0.005 eV/Å. The remaining layers of the slab are kept fixed at their ideal bulk positions. All slabs have been set up using a theoretical lattice constant of 4.18 Å. The slight overestimate compared to the experimental value of 4.08 Å is consistent with other density-functional calculations, e. g., for noble metals using GGA functionals.[72,73]

The final absolute chemisorption energies of BDT or BDTR configurations on Au(111) are calculated for a slab geometry comprising 9 layers of gold and a (4×3), (4×4), (4×6), (6×3), or (6×6) surface unit cell. The **k**-point meshes in the complete first Brillouin zone comprise 48, 36, 24, 32, and 16 special **k** points, respectively.[71] In case of BDT or BDTR on Au(100), the slab comprises 12 atomic layers and a (4×3), (4×4), or (6×6) surface unit cell. The **k**-point meshes in the complete first Brillouin zone comprise 48, 36, and 16 special **k** points, respectively. In both cases, the Kohn-Sham wave functions are expanded in a plane-wave basis set with a cutoff energy of 340 eV, and 1000 eV cutoff for the augmentation charge.

The convergence with respect to cutoff energy, **k**-point sampling, number of relaxed substrate layers and total number of substrate layers has been subject to systematic convergence tests as reported in Appendix C. In summary, the overall error of the reported absolute values of the binding energies with respect to these convergence parameters amounts to approximately 0.1 eV. The total-energy differences between chemisorption configurations are less susceptible to the choice of these parameters. The error induced by the use of the approximate PW91 exchange-correlation energy functional is not included in this estimate. The coverage dependence of the BDT or BDTR chemisorption energies (corresponding to different sizes of the surface unit cell) depends on surface orientation and will be detailed in Appendix B.

The program P4VASP (Ref. 74) has been used to visualize all atomic configurations and STM-images calculated within the Tersoff-Hamann approach.[75]

Finally, we have applied semi-empirical dispersion corrections in order to investigate the effect of van der Waals (vdW) corrections to the binding energies calculated within PW91-DFT.[76–78] Exchange-correlation functionals accounting for dispersion-interactions[79] are beyond the scope of the present paper. The semiempirical vdW correction is cut off at short range using a Fermi-function while the long range vdW interaction of atoms i and j is described by $s_6 C_{6,ij}/R_{ij}^6$.[77] In the literature s_6 has been chosen differently for different exchange-correlation functionals.[77] Here we have taken $s_6=0.75$, which is the value suggested by Grimme[77] in case of the closely related PBE exchange-correlation functional. The C_6 parameters are calculated from experimental atomic polarizabilities and ionization energies[108] by means of the London formula.[78,80] Experimental vdW-radii[109] are used to define a scale for the interatomic distances that enter the Fermi cutoff function.[81,82]

How to obtain an appropriate choice of above constants for the vdW interaction is certainly an issue, apart from the question how well the approach is suitable for metal surfaces. Recently Tkatchenko *et al.* proposed a method of deriving C_6 coefficients and vdW radii for atoms in molecules,

which results in smaller values for the C_6 coefficients and larger vdW radii.[76] To obtain a rough impression of the effect associated with such a variation of the parameters that control the vdW interaction, we artificially decreased the C_6 coefficients by approximately 20% and concomitantly increased the vdW radii between 20% and 50%. The variation of the vdW correction with respect to these parameter changes will be discussed in the main part of this work. To test the consistency of our vdW parameters we have applied them to the case of benzene adsorbed on Au(111). We found the adsorption energies for our original parameter set, and the scaled parameter set described above, to vary over about the same range of adsorption energies as the data presented by McNellis *et al.*.[83]

III. RESULTS AND DISCUSSION

A. Adsorption on Au(111)

The search for the ground-state adsorption configurations of BDT molecules and radicals is an important and indispensable prerequisite for any investigation concerning the growth properties of the adsorbed species. Beyond that, a detailed knowledge of competing configurations which are within a few k_bT of the ground state is almost equally important to facilitate a thorough study of diffusion.

In order to assess whether adsorbed BDT binds to the Au(111) surface as molecules or dissociates into BDTR and H_2, the chemisorption energy and ground-state configuration of both BDT and BDTR need to be calculated. Hence, in the following sections we discuss the submonolayer adsorption of BDT molecules and radicals on the defect-free, unreconstructed Au(111) surface. As previous DFT-studies of monothiol adsorption have revealed the importance of surface defects (Refs. 84–86), we present calculations for adsorbed BDT radicals in the presence of Au adatoms or surface vacancies.

1. Adsorption of BDT molecules on defect-free Au(111)

Local total-energy minima and the corresponding binding energies have been calculated for BDT adsorbed on the unreconstructed, but relaxed, Au(111) surface. A set of five initial configurations has been relaxed to local energy minima. The initial configurations differ by the number of S-Au bonds, which can be either one or two in case of BDT lying parallel to the surface, and the choice of the Au surface atoms to which the S atoms bind on top. Bonding to Au(111) hollow sites is expected to be of minor importance. A DFT-study conducted by Maksymovich *et al.* has shown that the HS-Au bond strength of methanethiol molecules $HSCH_3$ at Au(111) hollow sites is at least 0.24 eV less favorable compared to bonding atop Au surface atoms.[87]

The strength of the molecule-surface bond has been calculated as the difference between the total energy of the adsorbate-substrate system and the sum of the total energies of the unreconstructed Au(111) surface and BDT in the gas phase,

$$E_b = E_{total}\{\mathrm{BDT/Au(111)}\} - E_{total}\{\mathrm{Au(111)}\} - E_{total}\{\mathrm{BDT}\}. \quad (1)$$

In the energetically most favorable adsorption geometry for one molecule per (4×3) surface unit cell, the BDT adopts a lying-down configuration in which the alkane chain is slightly bent and the C-C-C planes of the molecule are oriented approximately parallel to the surface, see Figs. 1(a) and 1(b). Both sulfur atoms are close to Au on-top positions. The molecule-surface DFT-PW91 binding energy is calculated to be $E_b=-0.45$ eV. The zero-point energy correction is not included. Relaxed structural parameters of BDT are summarized in Table I.

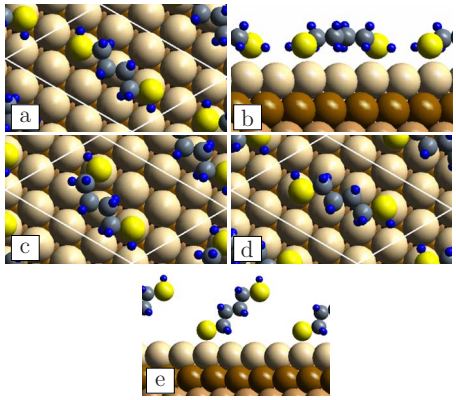

FIG. 1. (Color online) Top view (a) and side view (b) of the BDT ground-state configuration with the lowest calculated energy per (4×3) surface unit cell on the unreconstructed Au(111) surface (DFT-PW91 binding energy $E_b=-0.45$ eV). Competing stable configurations are shown for comparison: (c) $E_b=-0.40$ eV, (d) $E_b=-0.38$ eV, and (e) $E_b=-0.35$ eV. The surface unit cell is indicated by white lines.

Energetically slightly less favorable configurations with the alkane chain oriented parallel to the surface are shown in Figs. 1(c) and 1(d) for comparison. The energy difference with respect to the structure with the lowest calculated energy amounts to only 0.05 and 0.07 eV, respectively.

The semiempirical vdW correction to the binding energy at a coverage of one BDT per (4×3) surface unit cell amounts to −1.43, −1.36, and −1.33 eV for the configurations depicted in Figs. 1(a), 1(c), and 1(d), respectively. Using the artificially scaled vdW-radii together with the smaller C_6 coefficients, we obtain vdW corrections of −0.71 eV almost equal for all three configurations. If the intermolecular contribution to the vdW interaction is omitted from the summation, above semiempirical vdW correction to the binding energy amounts to −1.07, −1.03, and −1.09 eV in case of the original vdW parameters. These data indicate the range of values obtained for the vdW interaction when the empirical approach is applied. Most importantly, we note that the ground-state configuration does not change when the vdW energy is added to the DFT total energy.

We point out that, based on comparison to experiment, we distrust the absolute value of the vdW correction to the binding energy. Lavrich *et al.* conducted TDS experiments for adsorbed alkanethiols and alkanedithiols with varying alkane chain lengths on the Au(111) surface.[88] They observe two peaks in the TDS spectrum for BDT. The peak at lower desorption temperature is attributed to physisorbed BDT molecules, with a desorption energy barrier of 0.85 eV. Neglecting the small zero-point corrections, our estimated binding energy including semiempirical vdW corrections of −1.9 eV

TABLE I. Structural parameters and binding energies for BDT configurations on the unreconstructed Au(111) surface as depicted in Fig. 1. E_b is the DFT-PW91 binding energy per molecule defined in Eq. (1), $d_{S\text{-}S}$ is the distance between the S atoms, $d_{S\text{-}Au}$ are the S-Au bond lengths, and $d_{Au\text{-}Au}$ is the distance between the Au atoms to which the BDT binds. The value in parenthesis is the equilibrium distance between the respective Au atoms on the surface.

Configuration	Cell size	E_b (eV)	$d_{S\text{-}S}$ (Å)	$d_{S\text{-}Au}$ (Å)	$d_{Au\text{-}Au}$ (Å)
a	(4×4)	−0.50	6.67	2.75, 2.75	5.91 (5.91)
a	(4×3)	−0.45	6.68	2.78, 2.79	5.92 (5.91)
c	(4×3)	−0.40	5.48	2.76, 2.80	5.08 (5.12)
d	(4×3)	−0.38	6.87	3.00, 2.93	7.74 (7.81)
e	(4×3)	−0.35	6.95	2.67	
BDT (gas)			6.89		

(−1.2 eV in case of the artificially scaled vdW parameters) is substantially larger than above experimental desorption energy barrier. Apparently, the semiempirical equation overestimates the vdW correction in case of BDT/Au. Furthermore, Lavrich *et al.* estimated the contribution to the binding energy per CH_2-group of the alkane chain to yield approximately −64 meV.[88] We arrive at a vdW contribution to the binding energy of −0.2 eV (about −0.1 eV in case of the artificially scaled vdW parameters) per CH_2 group of the BDT molecule, which is considerably larger than the experimental estimate. Again, the vdW correction appears to be overestimated by the present semiempirical approach. The issue of the contribution from the vdW interaction to the binding energy is still an open question for molecules with alkane chains on metal surfaces. For clarity we will henceforth quote the unaltered DFT-PW91 binding energies in this paper.

Besides lying-down configurations an upright configuration has been calculated in which the alkane chain and one of the HS groups are pointing away from the surface [see Fig. 1(e)]. In this configuration only one S atom is located atop a Au surface atom forming an HS-Au bond with a binding energy of E_b=−0.35 eV. The tilt angle of the S-S axis with respect to the surface normal amounts to 56°. A rotation of the molecule around the surface normal through the S-Au bond has not been calculated because we expect the variation of the total energy with azimuthal angle to be insignificant. This we conclude from the work by Maksymovich *et al.* who considered the rotation of $HSCH_3$ molecules that bind to Au(111) in an atop configuration and who found an energy variation with azimuthal angle on the order of only 5 meV.[87] We will refer to the configuration shown in Fig. 1(e) as on-top upright.

We are not aware of other theoretical studies of adsorbed BDT molecules on Au(111) that we could directly compare to. There are, however, DFT calculations for the adsorption of methanethiol molecules $HSCH_3$ on Au(111).[87] The authors of Ref. 87 report an adsorption geometry for the $HSCH_3$ molecule that is similar to the on-top upright configuration of the BDT molecule with respect to the positions of the corresponding H, S, and C atoms. For the energetically most favorable structure, the calculated binding energy per $HSCH_3$ molecule is reported to be −0.37 eV and the S-Au bond length is reported to be 2.668 Å.[87] Within the accuracy of our calculations, both quantities agree with the respective values for the on top-upright configuration (see Table I). Lavrich *et al.* estimate the universal contribution of the SH group to the binding enthalpy for alkanethiols with varying lengths to be −0.35 eV from TDS experiments.[88] Neglecting zero-point corrections and omitting the semi-empirical vdW contributions to the HS-Au bond, this value is consistent with the calculated HS-Au bond strength from Ref. 87 and our bond strength for BDT in the on-top upright configuration.

2. Adsorption of BDT radicals on defect-free Au(111)

We calculate the adsorption of BDTR on the Au(111) surface in the absence of surface defects. The search for the ground-state configuration is complicated by intramolecular conformational degrees of freedom and the availability of two S-Au bonding sites which can result in many stable configurations being close-by in energy. Therefore, as many as 20 initial configurations have been relaxed to local total-energy minima. Since it is well established within DFT that the sulfur atoms of alkanethiol-radicals bind to the defect-free, unreconstructed Au(111) surface in the vicinity of Au(111) hollow sites (Refs. 60, 61, and 89–100), the initial configurations have been chosen such that both sulfur atoms are located either close to fcc-or hcp-hollow sites. This approach is supported by the fact that a configuration with both S atoms at Au(111) on-top sites proved to be unstable. For the majority of configurations the C atoms of the alkane chain are approximately located in a plane parallel to the Au(111) surface. This corresponds to the energetically most favorable conformation of free BDTR. In addition, three initial configurations with other conformations of BDTR have been chosen. Throughout this section the spin-polarized ground state of BDTR in vacuum is chosen as the energy reference $E_{total}^{spin}\{BDTR\}$ [see Eq. (1)].

Finally, a configuration with an inclined alkane chain and with only a single S-Au bond was calculated. The S atom is located at an fcc-bridge position. After relaxation, the binding energy amounts to −1.9 eV. This is consistent with the binding energy for adsorbed SCH_3 radicals on the unreconstructed Au(111) surface.[61]

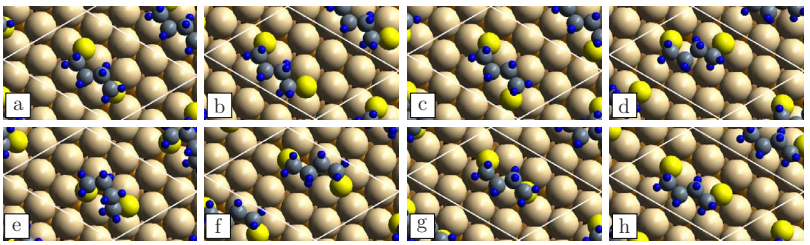

FIG. 2. (Color online) Top view of BDTR on the unreconstructed Au(111) surface. (a) Ground-state configuration with the lowest calculated binding energy (E_b=−3.26 eV) for the (4×3) and (4×4) surface unit cell. (b)–(h) Competing stable configurations with smaller absolute values of the binding energies, see Table II. The surface unit cell is indicated by white lines.

For a coverage of one BDTR per (4×3) and (4×4) surface unit cell the adsorption geometry in Fig. 2(a) yields the lowest total energy. The binding energy is E_b=−3.26 eV and E_b=−3.45 eV in case of the (4×3) and (4×4) surface unit cell, respectively. Evidently, the bond strength between BDTR and the Au(111) surface increases substantially as the coverage is decreased. We were not able to obtain the binding energy of an individual adsorbed BDTR even in case of a large (6×6) surface unit cell. This coverage dependence is attributed to strong substrate-mediated, adsorbate-adsorbate interactions, which we conclude from the data presented in Appendix B.

In the ground-state configuration both sulfur atoms bind to the substrate in the vicinity of fcc-hollow sites of Au(111). One of the S atoms is shifted by 0.57 Å toward a nearby bridge site, thus adopting a fcc-bridge position. The corresponding S-C bond is tilted with respect to the surface normal by 50°. The other sulfur atom binds at an fcc-site experiencing only a small shift of 0.06 Å toward a bridge site and a tilt of 13° of the S-C bond. Both S atoms adopt positions with respect to the substrate which resemble S-atom positions and S-C tilt angles of low adsorption-energy configurations of the SCH_3 radical on the Au(111) surface.[61]

In order to gain a deeper insight in to the nature of the BDTR-Au bond, we resort to the charge density difference $\Delta\rho(\mathbf{r})=\rho_{\mathrm{BDTR/Au(111)}}(\mathbf{r})-\rho_{\mathrm{BDTR}}(\mathbf{r})-\rho_{\mathrm{Au(111)}}(\mathbf{r})$. A distinct charge accumulation in the region between the S atoms and neighboring Au atoms is revealed which is indicative of the covalent S-Au bond formed upon adsorption. The partially filled HOMO orbitals of free BDTR are located at the S atoms and have a dominant 3*p* character. These *p* orbitals are oriented nearly perpendicular to the S-C bond, which favors tilted S-C bond orientations. From this we conclude, that the adsorbate-surface bond primarily originates from a hybridization of sulfur 3*p* states and substrate Au states.

The calculations reveal that the potential energy surface involves many local minima within a range of only a few 100 meV. This multivalley potential-energy landscape originates from the interplay between two S-Au adsorbate-surface bonds and the internal conformational degrees of freedom of BDTR. It differs fundamentally from the comparatively simple potential energy surface of a single SCH_3 radical which only form one S-Au bond with the Au(111) surface. An excerpt of competing stable configurations is depicted in Figs. 2(b)–2(h) and corresponding structural information is summarized in Table II. Among the calculated configurations, (a)–(f) represent the lowest-energy configurations. Interestingly, while (g) and (h) appear to have similar geometries as low-energy configurations, the absolute value of the binding energy is at least 0.18 eV smaller than for the ground-state configuration (a). A general characteristic of all calculated stable configurations is that both sulfur atoms bind to the substrate close to hollow or hollow-bridge sites.

Since it is a difficult task to locate the global minimum on a complicated potential energy surface, we provide an estimate for a lower bound of the global BDTR/Au(111) chemisorption energy in Appendix A. Altogether, we are confident that the configuration in Fig. 2(a) constitutes the ground state for submonolayer coverages of BDTR on the unreconstructed Au(111) surface. At worst, we expect it to be within a few k_BT of the global minimum at room temperature.

The semiempirical vdW correction is calculated in order to asses its impact on the conclusions drawn from relative binding energies of BDT molecules and radicals in Sec. III A 4. For the binding energy of the ground-state geometry in Fig. 2(a) it amounts to −1.33 and −1.37 eV in case of the (4×3) and (4×4) surface unit cell, respectively. Decreasing the C_6 coefficients and increasing the vdW radii as described in Sec. II yields a vdW correction of −0.68 and −0.70 eV. Notably, for both parameter sets the semiempirical vdW corrections for the BDT molecule and the BDT radical differ by less than 0.1 eV. Thus, the results presented in Sec. III A 4 based on binding energy differences between BDT molecules and BDT radicals are unaffected by the semiempirical vdW correction employed here. The same conclusions can be drawn in case of the Au(100) surface considered in Sec. III B. In order to quantify the effect of changes in bond distances due to vdW interactions on the STM-images, additional relaxations have been carried through. The ground-state configurations for BDT and BDTR on the Au(111) surface have been relaxed until the residual force per atom including the semiempirical vdW correction was smaller

TABLE II. Structural parameters and binding energies for an excerpt of calculated configurations of BDTR on the unreconstructed Au(111) surface as depicted in Fig. 2. E_b is the DFT-PW91 binding energy per radical as defined in Eq. (1) and $d_{S\text{-}S}$ refers to the distance between the S atoms. The approximate bonding sites of both S atoms are described in the last column.

Configuration	Cell size	E_b (eV)	$d_{S\text{-}S}$ (Å)	S-atom sites
a	(4×3)	−3.26	4.85	fcc-bridge, fcc
b	(4×3)	−3.25	5.48	fcc-, hcp-bridge
c	(4×3)	−3.24	5.44	fcc-, hcp-bridge
d	(4×3)	−3.23	4.81	fcc, fcc-bridge
e	(4×3)	−3.21	4.10	fcc, hcp-bridge
f	(4×3)	−3.19	5.41	fcc, fcc-bridge
g	(4×3)	−3.08	4.58	hcp, fcc
h	(4×3)	−3.05	5.28	fcc-, fcc-bridge

than 0.01 eV/Å. We observe no significant change of the calculated STM images.

3. Adsorption of BDT radicals in the presence of surface defects on Au(111)

In case of the adsorption of SCH_3 radicals on the unreconstructed Au(111) surface, geometries involving Au adatoms are found to be energetically favored compared to geometries without adatoms.[61,100–102] Furthermore, it has been reported that adsorption of $HSCH_3$ molecules at surface vacancies leads to a cleavage of the H-S bond and the formation of adsorbed alkanethiol radicals.[84–86] This has motivated us to investigate similar configurations in case of BDTR.

To assess the role of surface defects for the adsorption of BDTR, we calculate adsorption geometries involving one Au adatom and one or two surface vacancies per surface unit cell. The number of defects will be denoted by n. The binding energy per BDTR relative to the defect covered surface and a free radical is defined as

$$E_{b1} = E_{total}\{\text{BDTR}/n \cdot \text{defect}/\text{Au}(111)\} - E_{total}\{n \cdot \text{defect}/\text{Au}(111)\} - E_{total}^{spin}\{\text{BDTR}\}. \quad (2)$$

To account for defect formation, we calculate the energy of n defects at the surface,

$$E_{defect} = E_{total}\{n \cdot \text{defect}/\text{Au}(111)\} - E_{total}\{\text{Au}(111)\} - n \cdot E_{total}^{bulk}\{\text{Au}\}. \quad (3)$$

The Au chemical potential equals the energy per bulk atom $E_{total}^{bulk}\{\text{Au}\}$. Hence the binding energy per BDTR as compared to the defect-free unreconstructed Au(111) surface is

$$E_{b2} = E_{b1} + E_{defect}. \quad (4)$$

E_{b2} includes the energy expense necessary for defect formation and can be compared to the binding energies of BDTR presented in the previous subsection.

a. Adatoms. We consider a configuration in which a Au adatom is initially bound to the unreconstructed Au(111) surface at a fcc-site. A BDTR is added such that both S atoms form a bond with both the adatom and the surface. Adsorption geometries in which only one S atom binds to the adatom are energetically less favorable. Two stable configurations were calculated with the Au adatom either above a fcc-hollow or a bridge site of the Au(111) surface. The energetically most favorable configuration with the adatom above the fcc-hollow site is depicted in Fig. 3(a). The DFT-PW91 binding energy for one BDTR per (4×3) surface unit cell amounts to $E_{b1}=-3.85$ eV with respect to the adatom covered surface and $E_{b2}=-3.21$ eV with respect to the defect-free surface. Decreasing the coverage to one radical per (4×4) surface unit cell results in a slight increase of the bond strength to $E_{b1}=-3.87$ eV and $E_{b2}=-3.26$ eV. The energetical preference for adsorption at the defect-free surface amounts to 0.05 and 0.19 eV in case of the (4×3) and (4×4) surface unit cell, respectively. Hence, Au adatoms are of minor importance for submonolayer chemisorption of BDTR on the unreconstructed Au(111) surface.

b. Vacancies. The position of Au atoms which have been removed from the surface in order to create one or two vacancies are labeled 1–4 in Fig. 3(b). The depicted initial configuration of BDTR prior to relaxation corresponds to its ground-state configuration.

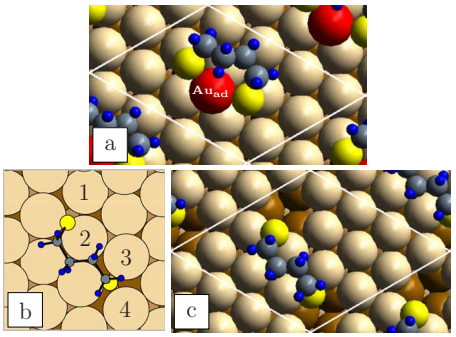

FIG. 3. (Color online) (a) Adsorption of BDTR at a Au adatom (red or dark gray) above a fcc-hollow site of the Au(111) surface ($E_{b2}=-3.21$ eV). Au atoms of the first layer: light gray or light brown, Au atoms of the second layer: dark gray or dark brown, and Au atoms of the third layer: gray or brown. (b) Schematic view of BDTR on the Au(111) surface in the ground-state configuration. Considered vacancy positions are labeled 1–4. (c) BDTR configuration with two surface vacancies at positions 1 and 4 ($E_{b2}=-3.15$ eV). The surface unit cells are indicated by white lines.

Among the considered geometries with only one vacancy, the energetically most favorable vacancy position is position 1. The DFT-PW91 binding energy as calculated in a (4×3) surface unit cell amounts to $E_{b1}=-3.81$ eV and $E_{b2}=-3.23$ eV. In case of the (4×4) surface unit cell, the binding energies are $E_{b1}=-3.88$ eV and $E_{b2}=-3.29$ eV.

BDTR configurations involving two vacancies have been calculated in a (4×4) surface unit cell in order to avoid that any two vacancies are located at nearest neighbor sites. The considered surface vacancy positions are (2,3) and (1,4). The largest absolute value of the binding energy per BDTR is obtained for vacancies at positions (1,4) as depicted in Fig. 3(c), with $E_{b1}=-4.35$ eV and $E_{b2}=-3.15$ eV.

Adsorption configurations involving one or two surface vacancies per (4×4) surface unit cell are energetically less favorable compared to adsorption at the defect-free Au(111) surface by at least 0.16 eV. Therefore, we expect that vacancies are not relevant for the submonolayer chemisorption of BDTR on the unreconstructed Au(111) surface.

4. S-H bond cleavage

The next section is devoted to the issue of BDT molecule dissociation via SH-bond cleavage and H_2 desorption into the gas phase. We make use of the DFT-PW91 binding energies of the optimum adsorption configurations of BDT and BDTR on the Au(111) surface. Thermodynamic equilibrium between BDT molecules, radicals, and hydrogen molecules in the gas phase is assumed. Metastable molecular chemisorption is not considered here.

In equilibrium, the relative abundance $p(\text{BDTR})/p(\text{BDT})$ of BDT radicals with respect to BDT molecules on the Au(111) surface is governed by the free energy difference,

$$\Delta f = [E_b\{\mathrm{BDTR}\} + f_{\mathrm{vib}}\{\mathrm{BDTR}\}] - [E_b\{\mathrm{BDT}\} + f_{\mathrm{vib}}\{\mathrm{BDT}\}] + E_{\mathrm{diss}}^{\mathrm{vac}} + [\mu_{\mathrm{H}_2}(T,p) - E_{\mathrm{total}}\{\mathrm{H}_2\}]. \quad (5)$$

$E_{\mathrm{total}}\{\mathrm{H}_2\}$ is the DFT total energy of an isolated hydrogen molecule. The dissociation of a free BDT into a BDTR and an H_2 molecule is endothermic by

$$E_{\mathrm{diss}}^{\mathrm{vac}} = E_{\mathrm{total}}\{\mathrm{BDTR}\} + E_{\mathrm{total}}\{\mathrm{H}_2\} - E_{\mathrm{total}}\{\mathrm{BDT}\}. \quad (6)$$

f_{vib} denotes the contribution per molecule to the vibrational free energy of a BDT molecule or radical adsorbed on the Au(111) surface. We approximate the difference $f_{\mathrm{vib}}\{\mathrm{BDT}\} - f_{\mathrm{vib}}\{\mathrm{BDTR}\}$ by the difference of zero-point energies of the BDT molecule and the BDT radical.

Vibrational frequencies have been determined using a finite difference approach as implemented in VASP. Atoms of the molecule are displaced by 0.025 Å in each direction of the Cartesian coordinate system. Diagonalization of the resulting approximation for the Hessian matrix yields the vibrational frequencies and the corresponding vibrational eigenmodes. For the H_2 molecule we obtain a zero-point energy of $\hbar\omega_{\mathrm{H}_2}/2 = 0.26$ eV. The difference of the zero-point energies between BDT and BDTR amounts to 0.55 eV.

The energy needed to break both S-H bonds of a free BDT is calculated to be 7.15 eV and the formation energy of H_2 amounts to −4.28 eV. In both cases zero-point energy-corrections are included. Thus, the dissociation of the free BDT molecule into a BDT radical and an H_2 molecule is endothermic by $E_{\mathrm{diss,zpc}}^{\mathrm{vac}} = 2.87$ eV including zero-point energies.

With the binding energies $E_b\{\mathrm{BDT}\} = -0.45$ eV and $E_b\{\mathrm{BDTR}\} = -3.26$ eV for a coverage of one BDT or BDTR per (4×3) surface unit cell, the free energy difference amounts to

$$\Delta f = 0.06 \text{ eV} + \left[\mu_{\mathrm{H}_2}(T,p) - E_{\mathrm{total}}\{\mathrm{H}_2\} - \frac{1}{2}\hbar\omega_{\mathrm{H}_2}\right]. \quad (7)$$

If the hydrogen reservoir is treated as an ideal gas, the chemical potential expression takes the form

$$\mu_{\mathrm{H}_2}(T,p) - E_{\mathrm{total}}\{\mathrm{H}_2\} - \frac{1}{2}\hbar\omega_{\mathrm{H}_2} = \tilde{\mu}_{\mathrm{H}_2}(T,p^0) + k_B T \ln(p/p^0). \quad (8)$$

p^0 is the reference pressure of 0.1 MPa. The temperature dependence of the chemical potential $\tilde{\mu}_{\mathrm{H}_2}(T,p^0)$ of hydrogen in the gas phase is taken from the thermodynamic tables of the CRC Handbook.[80] A similar logarithmic dependence is obtained in case of dilute solutions of H_2 in an electrolyte. At room temperature, the thermal energy $k_B T$ is only a factor of two to three smaller than the energy difference 0.06 eV in the above expression. Hence, the sign of Δf will change in favor of BDTR adsorption on the Au(111) surface at sufficiently small H_2 partial pressure. E.g., at a temperature of $T = 300$ K, and a hydrogen partial pressure as large as $p = 0.1$ MPa, adsorption of BDTR is still favorable compared to adsorbed BDT by approximately 0.26 eV. Thus, our calculations indicate that at submonolayer coverage the S-H bonds would be cleaved due to entropic reasons.

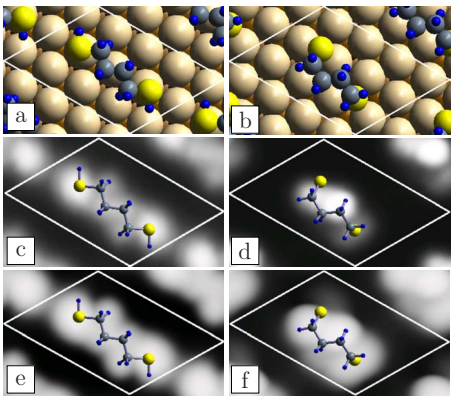

FIG. 4. (Color online) STM-images simulated within the Tersoff-Hamann model. The LDOS is integrated from the Fermi energy ε_F to $\varepsilon_F + 0.8$ eV. The underlying adsorption geometries of BDT and BDTR are depicted in (a) and (b). STM-images of the molecule in (c) and the radical in (d) are evaluated at a constant height of $\Delta z = 7$ Å above the Au surface atoms. Simulated constant-current STM-images of BDT (e) and BDTR (f) at a contour of $\rho_0 = 1.4\times10^{-5}$ e/Å^3. The (4×3) surface unit cell is indicated by white lines. Gray scales have been chosen independently in (c)–(f).

In addition, the question arises whether BDT molecules dissociate under UHV conditions, which is difficult to assess due to the large herringbone reconstruction of the Au(111) surface. One effect of this reconstruction is a partial relaxation of the surface stress by incorporating additional gold atoms into the surface. This effectively reduces the average Au-Au distance along the $[1\bar{1}0]$ direction within the first atomic layer by approximately 4%.[102,103] We have tried to simulate this higher density of Au surface atoms within the first layer by compressing our whole slab with the unreconstructed Au(111) surface in the $[1\bar{1}0]$ direction by 4%.[110] In case of BDTR, the main effect of the smaller Au-Au distance is a reduction of the bond strength of both S-Au bonds together by approximately 0.5 eV. On the other hand, the absolute value of the binding energy of BDT decreases only by approximately 0.1 eV. At hydrogen partial pressures of less than 0.1 MPa and $T = 300$ K, adsorption of BDTR on the compressed Au(111)(1×1) model surface is energetically slightly favored.

5. Simulated STM images

STM-images of adsorbed BDT and BDTR are simulated within the Tersoff-Hamann model (Ref. 75) for the energetically most favorable configurations (see Figs. 4(a) and 4(b)). To this purpose the local density of states (LDOS) is integrated from the Fermi energy ε_F to $\varepsilon_F + eU$ using different values for eU ranging from −1.8 to 0.8 eV. In Figs. 4(c) and 4(d) the integrated LDOS is evaluated at a constant height of $\Delta z = 7$ Å above the Au surface atoms. Constant current topographies at a contour level of $\rho_0 = 1.4\times10^{-5}$ e/Å^3 and eU = +0.8 eV are depicted in Fig. 4(e) for BDT and in Fig. 4(f) for BDTR.

The calculated constant height and constant-current images of BDT and BDTR exhibit elongated features with a major contribution originating from the alkane chain. In case

of BDT, the simulated STM image reflects the nearly symmetric conformation of the molecule at the surface. By contrast, the STM-images of adsorbed BDTR look asymmetric. This is a consequence of the two inequivalent S-Au bonds and a distortion of the alkane chain. Note that at finite temperatures the STM images might appear symmetric due to thermal averaging. Furthermore, application of Au(111)(1×1) two-dimensional space group transformations will result in isoenergetic chemisorption configurations.

Leung *et al.* have deposited 1,6-hexanedithiol molecules on the Au(111) surface and characterized the resulting adsorption geometries by low energy atom diffraction, grazing incidence x-ray diffraction, and STM measurements.[33] STM images reveal a striped phase of the adsorbed species manifested by elongated bright features which line up along high symmetry directions of the Au(111) surface.[33] The data is consistent with configurations in which the adsorbate is lying flat on the surface with the C-C-C plane approximately parallel to the substrate.[33] The alkane chain is proposed to point approximately in the $\langle 1\bar{1}0\rangle$ directions.[33] The bright features in the STM-images are suggested to originate from rows of S atoms of two adjacent molecules in the densely packed structure.[33]

A comparison to the calculated STM images appears rather difficult as we calculate shorter alkanedithiols at lower coverages. However, our data leads us to speculate that not only the S atoms but also the alkane chain contributes to the bright features observed in STM images.

B. Adsorption on Au(100)

In contrast to the close-packed Au(111) surface a more open surface such as Au(100) can lead to a stronger binding of adsorbates to surface atoms, e.g., in case of SCH_3 adsorption.[104,105] This is of particular interest, e.g., for Video-STM experiments, as stronger adsorbate-surface bonds can lead to lower diffusion rates which facilitate a direct observation of single diffusion events. In the following sections we calculate the ground-state configuration for BDT on the Au(100) surface and assess whether dissociation into BDTR and H_2 may occur.

1. Adsorption of BDT molecules on defect-free Au(100)

Local total-energy minima and the corresponding binding energies have been calculated for BDT adsorbed on the unreconstructed, but relaxed, Au(100) surface. A set of three initial configurations has been relaxed to local energy minima. In the initial configurations the BDT alkane chain is lying parallel to the surface. The molecule forms two S-Au bonds, with the S atoms located approximately atop Au surface atoms. Adsorption configurations with only a single S-Au bond are expected to be energetically unfavorable. This has been concluded without explicit computation by considering the binding energy of a single $HSCH_3$ molecule bonded atop a Au surface atom. In order to asses bonding to hollow sites, calculations were performed in which a single $HSCH_3$ molecule binds to a Au(100) hollow site. As a matter of fact, this configuration proved to be unstable. In the relaxed configuration the $HSCH_3$ molecule binds on top to a single Au surface atom. The on top binding energy E_b amounts to -0.45 eV.

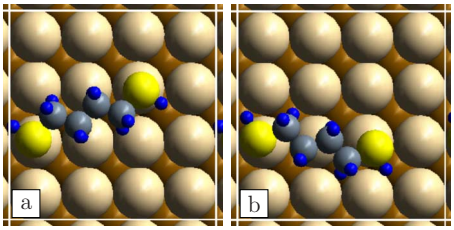

FIG. 5. (Color online) (a) BDT configuration with the largest absolute value of the binding energy per (4×4) surface unit cell of the unreconstructed Au(100) surface ($E_b=-0.77$ eV). (b) Competing configuration shown for comparison ($E_b=-0.72$ eV). The surface unit cell is indicated by white lines.

The energetically most favorable adsorption geometry for one BDT per (4×4) surface unit cell is shown in Fig. 5(a). Here the BDT molecule adopts a lying-down configuration in which the alkane chain is slightly bent and the C-C-C planes are oriented approximately parallel to the surface. Both sulfur atoms are close to Au on-top positions. The molecule-surface binding energy is calculated to be $E_b=-0.77$ eV not including zero-point energies. Structural parameters are summarized in Table III.

An energetically slightly less favorable configuration is shown in Fig. 5(b) for comparison. The energy difference with respect to the structure with the lowest calculated energy amounts to 0.05 eV in case of the (4×4) surface unit cell.

TABLE III. Structural parameters and binding energies for BDT configurations on the unreconstructed Au(100) surface as depicted in Fig. 5. E_b is the DFT-PW91 binding energy per molecule defined in Eq. (1), $d_{S\text{-}S}$ is the distance between the S atoms, $d_{S\text{-}Au}$ are the S-Au bond lengths, and $d_{Au\text{-}Au}$ is the distance between the Au atoms to which the BDT binds. The value in parenthesis is the equilibrium distance between the respective Au atoms. E_b for an inclined configuration is approximated by a $HSCH_3$ molecule adsorbed atop a Au surface atom.

Configuration	Cell size	E_b (eV)	$d_{S\text{-}S}$ (Å)	$d_{S\text{-}Au}$ (Å)	$d_{Au\text{-}Au}$ (Å)
a	(4×4)	−0.77	6.77	2.59, 2.59	6.63 (6.61)
b	(4×4)	−0.72	6.67	2.60, 2.60	5.89 (5.91)
b	(4×3)	−0.66	6.67	2.61, 2.61	5.89 (5.91)
$HSCH_3$ on top	(3×3)	−0.45		2.57	
BDT (gas)			6.89		

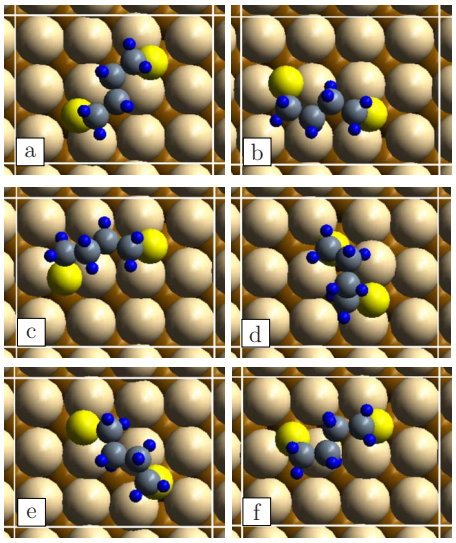

FIG. 6. (Color online) (a)–(c) BDTR configurations with the largest absolute value of the binding energy on the unreconstructed Au(100) surface. (d)–(f) Lowest energy competing configurations are shown for comparison. The surface unit cell is indicated by white lines.

Compared to adsorption on the Au(111) surface, BDT binds stronger to the Au(100) surface by approximately 0.27 eV for a coverage of one molecule per (4×4) surface unit cell. The lower binding energy on the Au(100) surface is also manifested in a shortening of the S-Au bond by approximately 0.15 Å. A weaker adsorbate-surface bond in case of denser-packed surfaces like the Au(111) surface is also observed for other adsorbates such as the SCH_3 radical (Ref. 104) or the $HSCH_3$ molecule.

2. Adsorption of BDT radicals on defect-free Au(100)

Energy minima for BDTR on the Au(100) surface were calculated by relaxing ten initial configurations to a local total-energy minimum. The initial configurations have been chosen such that both S atoms of the radical are located near hollow sites of the Au(100) substrate. Configurations in which either S atom is located atop Au surface atoms have not been taken into consideration as an initial starting geometry. Calculations for an adsorbed SCH_3 radical on the Au(100) surface reveal that on top positions of the S atom are unstable. Within this survey the alkane chain of the BDT radical has been oriented approximately parallel to the surface for all but two considered initial configurations.

Calculations for this survey have been carried through for a coverage of one BDTR per (4×3) surface unit cell. We found the adsorption geometries depicted in Figs. 6(a)–6(c) to have the lowest total energy among all other configurations. The configurations are calculated to be energetically degenerated to within 10 meV. The corresponding DFT-PW91 binding energies are $E_b=-4.01$, -4.02, and -4.01 eV, for Figs. 6(a)–6(c), respectively. The bond between BDTR and the Au surface strengthens as the coverage decreases to one radical per (4×4) surface unit cell. Thus, the binding energy decreases to $E_b=-4.11$, -4.09, and -4.07 eV for the adsorption configurations depicted in Figs. 6(a)–6(c), respectively. The small, almost coverage independent energy splitting of 10–30 meV between these configurations is not considered to be significant, see Appendix B.

TABLE IV. Structural parameters and binding energies for an excerpt of calculated configurations of BDTR on the Au(100) surface as depicted in Fig. 6. E_b is the DFT-PW91 binding energy per radical as defined in the main text, and $d_{S\text{-}S}$ refers to the distance between the S atoms.

Configuration	Cell size	E_b (eV)	$d_{S\text{-}S}$ (Å)
a	(4×3)	−4.01	5.36
b	(4×3)	−4.02	5.33
c	(4×3)	−4.01	5.45
d	(4×3)	−3.93	3.92
e	(4×3)	−3.93	5.39
f	(4×3)	−3.91	5.06

Both sulfur atoms of the BDTR bind to the Au(100) surface in between hollow and bridge sites (hollow-bridge separation equal to 1.48 Å). The S atoms are shifted from the hollow site to a nearby bridge site by 0.8 Å in Fig. 6(a), 1.2 and 0.9 Å in Fig. 6(b), as well as 1.1 and 0.9 Å in Fig. 6(c). As in the case of low-energy adsorption configurations of single SCH_3 radicals (Ref. 105), both SCH_2 groups of BDTR bind in tilted hollow-bridge like configurations to the Au(100) surface. The tilt angles with respect to the surface normal amount to 34° in Fig. 6(a), 53° and 30° in Fig. 6(b), and 53° and 41° in Fig. 6(c).

An excerpt of competing configurations for one BDTR per (4×3) surface unit cell of the Au(100) surface is depicted in Figs. 6(d)–6(f). Corresponding structural information is summarized in Table IV. Among the calculated configurations, (a)–(f) represent the four lowest-energy configurations. In all relaxed configurations both sulfur atoms bind to the substrate close to hollow- or bridgelike sites.

Our calculations again reveal the appearance of a multivalley structure of the potential energy surface. As in the case of Au(111), we find local minima which are within a range of only a few 100 meV. Notably, in case of the Au(100) surface the interplay between two S-Au bonds of the radical and the BDTR internal degrees of freedom leads to three inequivalent configurations, which are very close in energy and, within the accuracy of the calculation, represent the ground state. This result plays an important role for the diffusion characteristics of BDTR on Au(100).

3. Adsorption of BDT radicals in the presence of surface defects on Au(100)

a. Adatoms. Two stable adsorption geometries have been calculated in which both S atoms of BDTR bind to a Au adatom and atop to Au atoms of the Au(100) surface. The configurations differ in the position of the adatom with respect to the underlying substrate, which has initially been chosen as either a bridge or a hollow position. Figure 7(a) depicts the lower total-energy configuration in which the

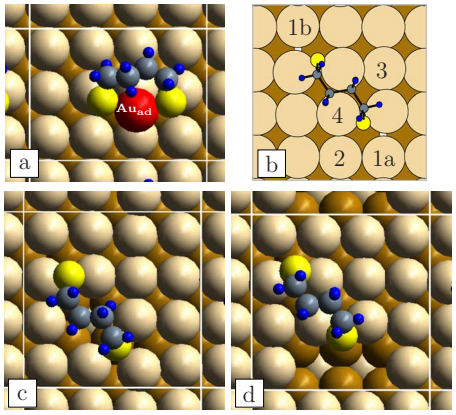

FIG. 7. (Color online) (a) Configuration involving one Au adatom (dark gray or red, E_{b2}=−3.46 eV). Au atoms of the first and third layer: light gray or light brown, Au atoms of the second layer: dark gray or dark brown. (b) Schematic representation of the lowest-energy BDTR configuration on the Au(100) surface. Considered defect positions are labeled 1a, 1b, 2, 3, and 4. (c) Configuration involving one surface vacancy at position 4 (E_{b2}=−4.05 eV). (d) Configuration involving two surface vacancies at position (1a, 2) (E_{b2}=−3.97 eV). The surface unit cell is indicated by white lines.

adatom is located near a bridge site. The DFT-PW91 binding energy E_{b2} with respect to the defect-free and unreconstructed Au(100) surface, defined in Eq. (4), amounts to E_{b2}=−3.46 eV for a coverage of one BDTR per (4×3) surface unit cell. Thus, the absolute value of the binding energy is approximately 0.56 eV smaller compared to the lowest-energy configurations on the defect-free surface with a binding energy of −4.02 eV. As a result, Au adatoms are not relevant for BDTR chemisorption on Au(100).

b. Vacancies. Adsorption configurations with one or two surface vacancies have been calculated in a (4×4) surface unit cell. The considered vacancy positions are labeled 1a, 1b, 2, 3, and 4 in Fig. 7(b). Initially the atomic coordinates of the BDT radical correspond to the lowest total-energy configuration on the defect-free Au(100) surface as depicted in Fig. 6(a).

For configurations involving a single surface vacancy one of the Au atoms labeled 1a, 3, or 4 is removed. In case of a vacancy at position 4, an alternative initial configuration of BDTR has been chosen in which both S atoms are located at the vacancy prior to relaxation. The Au atoms labeled (1a,1b) or (1a,2) have been removed for configurations involving two vacancies.

Figures 7(c) and 7(d) show the energetically most favorable configurations with one or two surface vacancies, respectively. The highest absolute value of the DFT-PW91 binding energy amounts to E_{b2}=−4.05 eV and occurs in case of one vacancy at position 4. We obtain E_{b2}=−3.97 eV in case of two vacancies at position (1a,2). In any case, the absolute value of the binding energy is at least 0.06 eV smaller compared to the lowest-energy configuration on the defect-free surface with a binding energy of −4.11 eV.

Configurations of BDTR on the unreconstructed Au(100) surface with vacancies are energetically less favorable compared to configurations without defects by at least two to three k_bT at room temperature. Based on this result, configurations with defects are expected to be of minor importance.

4. S-H bond cleavage

In the previous sections we discussed the chemisorption energetics of both BDT molecules and radicals on the unreconstructed Au(100) surface. For a coverage of one BDT per (4×4) surface unit cell we obtained DFT-PW91 binding energies for the optimum configurations of −0.77 eV in case of the molecule and −4.11 eV for the radical. As stated in Sec. III A 4, the energy needed to cleave both S-H bonds of BDT and subsequently form H_2 amounts to −2.87 eV including zero-point energy corrections. Thus, the relative abundance $p(\mathrm{BDTR})/p(\mathrm{BDT})$ of BDT radicals with respect to BDT molecules on the unreconstructed Au(100) surface is governed by the free energy difference,

$$\Delta f = -0.47\ \mathrm{eV} + \left[\mu_{H_2}(T,p) - E_{\mathrm{total}}\{H_2\} - \frac{1}{2}\hbar\omega_{H_2}\right]. \quad (9)$$

Evidently, a cleavage of both S-H bonds and subsequent H_2 formation is already energetically favored at a temperature of 0 K by approximately 0.47 eV in case of BDT adsorbed on Au(100). This distinct tendency toward dissociation into BDTR and H_2 is further assisted by entropy effects as described in Sec. III A 4.

IV. SUMMARY

Synthesis of organic molecular assemblies at surfaces and surface functionalization can be achieved by binding organic molecules to metal surfaces via thiol groups.[2] Here we present DFT calculations for the submonolayer adsorption of BDT molecules [BDT: HS-$(CH_2)_4$-SH] and BDT radicals [BDTR: ·S-$(CH_2)_4$-S·] on the (111) and (100) surfaces of gold. Dithiols on Au surfaces are an intensely studied model system for sulfur bonded organic molecules with promising perspectives in molecular electronics.[12–14,33] We adsorb the molecules on the unreconstructed Au(111) and Au(100) surfaces, which can be stabilized in an electrochemical environment.[47,48]

BDTR adsorption on Au surfaces differs fundamentally from the adsorption of mono-thiols with only a single S-Au bond. The presence of two S-Au molecule-surface bonds—together with the internal conformation degrees of freedom of the molecule—results in a complicated multivalley potential-energy surface. Identification of the adsorbed species—BDT or BDTR—and their lowest-energy adsorption configurations is an indispensable prerequisite for the study of diffusion and growth of BDT molecular films. Our results suggest a much more versatile phenomenology for adsorption and diffusion than described previously in case of the monothiols.[61]

While DFT total-energy differences come out 0.06 eV in favor of chemisorbed BDT molecules at a coverage of one molecule per (4×3) Au(111) surface unit cell, inclusion of entropic effects results in S-H bond cleavage. Thus, in equilibrium, BDT radicals are expected to be the dominant species on the unreconstructed Au(111) surface. On Au(100)

BDT radicals are found to be the energetically preferred species.

Both for Au(111) and Au(100) the BDT radicals adopt a lying-down configuration in which both sulfur atoms bond to Au surface atoms in hollow or bridgelike positions. Irrespective of the chosen surface orientation, Au(111) or Au(100), local energy minima are found to exist within a few 100 meV of the ground-state configuration. In case of Au(100) we found lowest-energy adsorption configurations, which come out energetically degenerate within the accuracy of the calculation. At a coverage of one radical per (4×4) and (6×6) surface unit cell the energy difference amounts to less than 0.03 eV.

As opposed to the adsorption of alkanethiols on Au(111), which has been observed experimentally[101] as well as theoretically[61,100,102] to become energetically more favorable in the presence of Au adatoms, we found no such energetical preference in case of BDT radicals on Au(111) or Au(100), neither for Au adatoms nor for Au surface vacancies.

Semiempirical vdW corrections to the binding energy have been evaluated. In case of the structures considered in this work, the ground-state configuration remained unaltered. In view of the absolute value of the vdW correction in comparison to experiment, however, a more sophisticated approach to vdW interactions appears to be required. Hence, plain DFT-PW91 binding energies have been quoted in this paper.

Constant current and constant height STM-images have been derived within the Tersoff-Hamann model (Ref. 75) for BDT molecules and radicals on the unreconstructed Au(111) surface. They exhibit elongated features at the position of the alkane chain, with the long axis approximately parallel to the chain. The long axis is slightly tilted with respect to the $\langle 1\bar{1}0\rangle$ directions.

ACKNOWLEDGMENTS

We thank O. Magnussen and K. Suto for helpful discussions and communication of experimental results prior to publication. We are grateful to A. Groß and K. Tonigold for stimulating discussions of their DFT results on the adsorption of dithiolates on gold surfaces. This work has been supported financially by the Deutsche Forschungsgemeinschaft (DFG) within Project No. Pe497/4-1. Calculations have been carried through at the Rechenzentrum der Universität Kiel.

APPENDIX A: ESTIMATED LOWER BOUND ON THE BDTR/AU(111) CHEMISORPTION ENERGY

In case of a complex potential energy landscape with multiple local minima it is a notoriously difficult problem to locate the global energy minimum. Our initial configurations, which we have relaxed into local potential energy minima, have been chosen by chemical intuition. Here we will try to provide an estimate for a lower bound of the binding energy per BDTR. The main contributions to the binding energy arise from the S-Au bonds, the conformational change of BDTR, the interaction of the alkane chain with the substrate, and substrate relaxation. At finite coverage, there are direct as well as substrate-mediated adsorbate-adsorbate interactions.

The energy needed to change the conformation of BDTR decreases the absolute value of the binding energy. A rather conservative approach is to omit this contribution to the binding energy. Typical energies associated with conformational changes are calculated to be order of 0.01–0.1 eV. We neglect the interaction of the alkane chain with the substrate. To obtain an approximate lower bound of the S-Au interaction, including the substrate relaxation and substrate-mediated adsorbate-adsorbate interactions, we have performed calculations for a (4×3) and (4×4) surface unit cell with two SCH_3 radicals adsorbed at the Au(111) surface. The initial position of the S atoms and the orientation of the S-C bonds have been adopted from the corresponding atoms of the BDTR ground-state configuration. Subsequently, a structural relaxation of both SCH_3 radicals and the substrate atoms was carried through. As a result, we obtain a binding energy per (4×3) and (4×4) surface unit cell for both SCH_3 radicals together of −3.47 and −3.57 eV, respectively. We take these values as a rough lower bound to the binding energy per BDTR for the respective surface unit cells. Notably, the calculated BDTR binding energies are only 0.2 and 0.1 eV above this bound. Due to the geometrical constraints in case of BDTR adsorption as opposed to the relaxation of two SCH_3 radicals, and in view of energies of the order of 0.01–0.1 eV associated with conformation changes of the free BDTR, we are confident that the calculated lowest-energy configuration in Fig. 2(a) is the ground-state configuration for submonolayer coverages of BDTR/Au(111). At worst, we expect our calculated optimum structure to be within a few k_BT of the global binding energy minimum at room temperature.

APPENDIX B: COVERAGE DEPENDENCE OF THE BDTR CHEMISORPTION ENERGY

1. Au(111)

The bond strength between BDTR and the Au(111) surface increases substantially with decreasing coverage Θ, as can been read from Table V. Due to prohibitive computational costs for calculations involving large surface unit cells we were not able to obtain the binding energy of an individual adsorbed BDTR, i.e., the limit $\Theta\rightarrow0$ could not be reached. We attribute the coverage dependence of the binding energy to strong substrate-mediated, adsorbate-adsorbate interactions. In order to corroborate this assertion, we relate the change in binding energy between the (4×3) and (4×4) surface unit cell to a quantitative measure of the change in adsorbate induced substrate relaxation. We observe that the effect of the sulfur-surface bond is an expansion of the hollow site in the vicinity of the S atom. Thus, the mutual distance $d_{i,j}$ of the neighboring three Au atoms is increased as compared to the clean substrate. We find that the expansion of the hollow sites increases as the coverage decreases.

In an effort to quantify this effect, we consider the sum of the distances between the Au atoms of the hollow sites which are closest to the S atoms for a given surface unit cell and BDTR configuration. The change of this quantity upon in-

TABLE V. Coverage dependence of structural parameters and binding energies for the configurations of BDTR/Au(111) in Fig. 2 and BDTR/Au(100) in Fig. 6. E_b is the DFT-PW91 binding energy per radical as defined in Eq. (1) and $d_{S\text{-}S}$ refers to the distance between the S atoms.

Configuration	Cell size	E_b (eV)	$d_{S\text{-}S}$ (Å)
	BDTR/Au(111)		
a	(4×3)	−3.26	4.85
a	(4×4)	−3.45	4.82
a	(4×6)	−3.63	4.83
a	(6×3)	−3.47	4.91
a	(6×6)	−3.72	4.85
b	(4×3)	−3.25	5.48
b	(4×4)	−3.31	5.50
c	(4×3)	−3.24	5.44
c	(4×4)	−3.29	5.44
d	(4×3)	−3.23	4.81
d	(4×4)	−3.31	4.86
	BDTR/Au(100)		
a	(4×3)	−4.01	5.36
a	(4×4)	−4.11	5.33
a	(6×6)	−4.18	5.33
b	(4×3)	−4.02	5.33
b	(4×4)	−4.09	5.31
b	(6×6)	−4.17	5.32
c	(4×3)	−4.01	5.45
c	(4×4)	−4.07	5.46
c	(6×6)	−4.15	5.46

creasing the surface unit cell from (4×3) to (4×4) is defined as

$$\Delta d = \sum_{\substack{i,j=1 \\ i<j}}^{3} [d_{i,j}^{(4\times4)}(S_1) + d_{i,j}^{(4\times4)}(S_2)] - \sum_{\substack{i,j=1 \\ i<j}}^{3} [d_{i,j}^{(4\times3)}(S_1) + d_{i,j}^{(4\times3)}(S_2)] \quad \text{(B1)}$$

S_1 and S_2 refer to the sulfur atoms of BDTR. In Fig. 8 we plot the change in binding energy versus Δd for different configurations. Clearly, a correlation between the increase in binding energy and the change of adsorbate induced substrate relaxations can be observed, which corroborates our assertion.

2. Au(100)

In contrast to the Au(111) surface the coverage dependence of the binding energy is less pronounced, see Table V. The absolute value of the binding energy increases by approximately 0.16 eV if the coverage is decreased from one BDTR per (4×3) surface unit cell to one BDTR per (6×6). In case of the Au(111) surface the increase of the absolute value of the binding energy amounts to 0.46 eV. Concomitantly, we find the adsorbate induced relaxation of the Au surface atoms in the neighborhood of the S atoms to depend much more sensitively on the size of the surface unit cell in case of the densely packed Au(111) surface as opposed to the more open Au(100) surface. In view of the correlation shown in Fig. 8 this is consistent with a stronger variation of the BDTR binding energy with surface unit-cell size in case of Au(111) as opposed to Au(100).

TABLE VI. Convergence of the binding energy E_b for BDTR on Au(111) in the configuration depicted in Fig. 2(a). The coverage corresponds to one BDTR per (4×3) surface unit cell. Note that the values for E_b in the main part of this work have been obtained with a cutoff energy of 340 eV, nine Au layers, and 48 **k** points.

E_{cutoff} (eV)	N_{kpt}	N_{layer}	$E_{xc}[n]$	E_b (eV)
		Plane wave cutoff energy E_{cutoff}		
250	12	4	GGA	−3.34
340	12	4	GGA	−3.39
420	12	4	GGA	−3.40
520	12	4	GGA	−3.41
		Number of Au layers N_{layer}		
250	12	4	GGA	−3.34
250	12	6	GGA	−3.37
250	12	9	GGA	−3.28
250	12	12	GGA	−3.29
250	12	15	GGA	−3.25
250	12	18	GGA	−3.26
		Number of *k*-points N_{kpt}		
250	12	4	GGA	−3.34
250	48	4	GGA	−3.26
250	108	4	GGA	−3.26
		Approx. to the $E_{xc}[n]$ functional		
250	12	4	GGA	−3.34
250	12	4	LDA	−4.96

APPENDIX C: CONVERGENCE TESTS

We report the convergence of the DFT binding energies of BDTR on the Au(111) and Au(100) surfaces with respect to computational parameters. The variation of binding energy due to an increase of the size of the surface unit cell (i.e., decrease of BDTR coverage) is discussed in Appendix B. In order to obtain an impression of the error related to the exchange-correlation functional $E_{xc}[n]$, we compare our GGA results to data calculated within the local density approximation (LDA) for $E_{xc}[n]$.[106,107]

TABLE VII. Convergence of the energy difference ΔE between different local chemisorption energy minima on the Au(111) surface.

Cell size	Config. in Fig. 2	E_{cutoff} (eV)	N_{kpt}	N_{layer}	$E_{\text{xc}}[n]$	ΔE (eV)
(4×3)	$a\leftrightarrow b$	250	12	4	GGA	0.041
(4×3)	$a\leftrightarrow b$	340	48	9	GGA	0.014
(4×3)	$a\leftrightarrow b$	250	12	4	LDA	−0.006
(4×4)	$a\leftrightarrow b$	250	9	4	GGA	0.109
(4×4)	$a\leftrightarrow b$	340	36	9	GGA	0.136
(4×3)	$a\leftrightarrow c$	250	12	4	GGA	0.047
(4×3)	$a\leftrightarrow c$	340	48	9	GGA	0.017
(4×4)	$a\leftrightarrow c$	250	9	4	GGA	0.131
(4×4)	$a\leftrightarrow c$	340	36	9	GGA	0.163
(4×3)	$a\leftrightarrow e$	250	12	4	GGA	0.073
(4×3)	$a\leftrightarrow e$	340	48	9	GGA	0.050
(4×3)	$a\leftrightarrow g$	250	12	4	GGA	0.180
(4×3)	$a\leftrightarrow g$	340	48	9	GGA	0.177
(4×3)	$a\leftrightarrow g$	250	12	4	LDA	0.226
(4×3)	$a\leftrightarrow h$	250	12	4	GGA	0.192
(4×3)	$a\leftrightarrow h$	340	48	9	GGA	0.206
(4×3)	$a\leftrightarrow h$	250	12	4	LDA	0.167

1. Au(111)

The convergence of the binding energy E_b per BDTR for the configuration depicted in Fig. 2(a) is summarized in Table VI. The error of E_b related to the cutoff energy of the plane-wave expansion, the number of Au layers in the slab, and number of **k**-points are estimated to be 0.02, 0.02, and less than 0.01 eV, respectively. An increase of the vacuum region thickness by ≈9 Å changes E_b by only 0.01 eV. As outlined in Sec. II, the relaxed positions of the Au atoms within the first three layers of the slab and the positions of the atoms of the BDT adsorbate are calculated in a slab comprising 4 layers of Au, a cutoff energy of 250 eV, and 12 special **k** points in the complete first Brillouin zone. Performing a relaxation of the atomic positions in a slab comprising 9 Au layers, a cutoff energy of 340 eV, and 48 special **k** points leads to an increase of the absolute value of E_b by less than 0.03 eV. Increasing the number of relaxed Au substrate layers from 3 to 5 changes the binding energy for one BDTR per (4×4) surface unit cell by approximately 0.01 eV

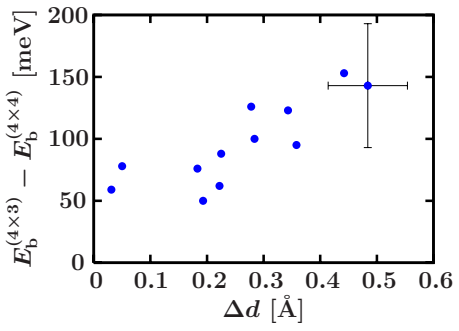

FIG. 8. (Color online) Change in binding energy E_b upon increasing the surface unit cell from (4×3) to (4×4) as a function of Δd for different configurations. Δd serves as a measure for the change in adsorbate induced substrate relaxations [see Eq. (B1)]. The data have been obtained using 250 eV for the cutoff energy, 12 **k** points in the full Brillouin zone, and 4 Au substrate layers.

TABLE VIII. Convergence of the binding energy E_b for BDTR on Au(100) in the configuration depicted in Fig. 6(b). The coverage corresponds to one BDTR per (4×3) surface unit cell. Note that the values for E_b in the main part of this work have been obtained with a cutoff energy of 340 eV, 12 Au layers, and 48 **k** points.

E_{cutoff} (eV)	N_{kpt}	N_{layer}	$E_{\text{xc}}[n]$	E_b (eV)
Number of Au layers N_{layer}				
250	12	4	GGA	−4.11
250	12	6	GGA	−4.00
250	12	10	GGA	−4.06
250	12	12	GGA	−4.03
250	12	14	GGA	−4.02
Number of k-points N_{kpt}				
250	12	4	GGA	−4.11
250	48	4	GGA	−4.07
250	108	4	GGA	−4.06
Approx. to the $E_{\text{xc}}[n]$ functional				
250	12	4	GGA	−4.11
250	12	4	LDA	−5.87

TABLE IX. Convergence of the energy difference ΔE between different (local) chemisorption energy minima on the Au(100) surface.

Cell size	Config. in Fig. 6	E_{cutoff} (eV)	N_{kpt}	N_{layer}	$E_{\text{xc}}[n]$	ΔE (eV)
(4×3)	$a\leftrightarrow b$	250	12	4	GGA	−0.018
(4×3)	$a\leftrightarrow b$	340	48	12	GGA	−0.009
(4×3)	$a\leftrightarrow b$	250	12	4	LDA	−0.069
(4×4)	$a\leftrightarrow b$	250	9	4	GGA	0.013
(4×4)	$a\leftrightarrow b$	340	36	12	GGA	0.014
(4×3)	$a\leftrightarrow c$	250	12	4	GGA	0.117
(4×3)	$a\leftrightarrow c$	340	48	12	GGA	0.084
(4×3)	$a\leftrightarrow d$	250	12	4	GGA	0.103
(4×3)	$a\leftrightarrow d$	340	48	12	GGA	0.100

(data for 250 eV cutoff energy, 12 **k** points, 9 Au layers in the slab).

Altogether, we arrive at an estimate for the absolute binding-energy error of approximately 0.10 eV not taking into account errors related to the use of the PW91-GGA exchange-correlation functional.

It is well known that the LDA for $E_{\text{xc}}[n]$ tends to overbind. Using the LDA, we obtain an absolute value of the binding energy which is 1.62 eV larger compared to PW91-GGA (see Table VI.

In Table VII the convergence of total-energy differences ΔE between different chemisorption configurations of BDTR on the Au(111) surface is summarized. The error of ΔE related to the cutoff energy, number of Au layers in the slab, and number of special **k** points is on the order of 0.03 eV.

The error of structural parameters like $d_{\text{S-S}}$ and $d_{\text{S-Au}}$ associated with a finite cutoff energy, number of Au layers in the slab, and number of special **k** points is estimated to be 0.02 Å.

2. Au(100)

The convergence of the binding energy E_{b} per BDTR for the configuration depicted in Fig. 6(b) is summarized in Table VIII. The error of E_{b} related to the number of Au layers in the slab and the number of **k**-points is estimated to be 0.01 eV each. We assume that the error of E_{b} related to the cutoff energy does not depend sensitively on surface orientation. Thus, we assume it to be equal to 0.02 eV. An increase of the vacuum region to ≈21 Å results in a change in E_{b} of 0.002 eV.

As outlined in Sec. II, the relaxed positions of the Au atoms within the first three layers of the slab and the positions of the atoms of the BDT adsorbate are calculated in a slab comprising 4 layers of Au, a cutoff energy of 250 eV, and 12 special **k** points in the complete first Brillouin zone. Performing a relaxation of the atomic positions in a slab comprising 12 Au layers, a cutoff energy of 340 eV, and 48 special **k**-points leads to a decrease of E_{b} by less than 0.03 eV.

Altogether, we arrive at an estimate for the absolute binding-energy error of approximately 0.09 eV not taking into account errors related to the use of the PW91-GGA exchange-correlation functional.

Using the LDA functional for $E_{\text{xc}}[n]$, we obtain a binding energy which is 1.77 eV lower compared to the PW91-GGA value (see Table VI).

In Table IX the convergence of the total-energy difference ΔE between different BDTR chemisorption configurations on the Au(100) surface is summarized. The error of ΔE related to the cutoff energy, number of Au layers in the slab, and number of special **k**-points amounts to ≈0.03 eV.

*franke@theo-physik.uni-kiel.de

[1] C. Joachim, J. K. Gimzewski, and A. Aviram, Nature (London) **408**, 541 (2000).
[2] F. Schreiber, J. Phys.: Condens. Matter **16**, R881 (2004).
[3] B. Baisch, D. Raffa, U. Jung, O. M. Magnussen, C. Nicolas, J. Lacour, J. Kubitschke, and R. Herges, J. Am. Chem. Soc. **131**, 442 (2009).
[4] Y. Wang, J. Kröger, R. Berndt, and W. A. Hofer, J. Am. Chem. Soc. **131**, 3639 (2009).
[5] M. Alemani, S. Selvanathan, F. Ample, M. V. Peters, K.-H. Rieder, F. Moresco, C. Joachim, S. Hecht, and L. Grill, J. Phys. Chem. C **112**, 10509 (2008).
[6] C. Dri, M. V. Peters, J. Schwarz, S. Hecht, and L. Grill, Nat. Nanotechnol. **3**, 649 (2008).
[7] A. S. Kumar, T. Ye, T. Takami, B.-C. Yu, A. K. Flatt, J. M. Tour, and P. S. Weiss, Nano Lett. **8**, 1644 (2008).
[8] M. Alemani, M. V. Peters, S. Hecht, K.-H. Rieder, F. Moresco, and L. Grill, J. Am. Chem. Soc. **128**, 14446 (2006).
[9] B.-Y. Choi, S.-J. Kahng, S. Kim, H. Kim, H. W. Kim, Y. J. Song, J. Ihm, and Y. Kuk, Phys. Rev. Lett. **96**, 156106 (2006).
[10] M. J. Comstock, N. Levy, A. Kirakosian, J. Cho, F. Lauterwasser, J. H. Harvey, D. A. Strubbe, J. M. J. Fréchet, D.

Trauner, S. G. Louie, and M. F. Crommie, Phys. Rev. Lett. **99**, 038301 (2007).
[11] J. Lahann, S. Mitragotri, T.-N. Tran, H. Kaido, J. Sundaram, I. S. Choi, S. Hoffer, G. A. Somorjai, and R. Langer, Science **299**, 371 (2003).
[12] D. L. Klein, R. Roth, A. K. L. Lim, A. P. Alivisatos, and P. L. McEuen, Nature (London) **389**, 699 (1997).
[13] M. A. Reed, C. Zhou, C. J. Muller, T. P. Burgin, and J. M. Tour, Science **278**, 252 (1997).
[14] J. G. Kushmerick, D. B. Holt, J. C. Yang, J. Naciri, M. H. Moore, and R. Shashidhar, Phys. Rev. Lett. **89**, 086802 (2002).
[15] F. Schreiber, Prog. Surf. Sci. **65**, 151 (2000).
[16] Q. Sun, A. Selloni, and G. Scoles, ChemPhysChem **6**, 1906 (2005).
[17] R. B. Pontes, F. D. Novaes, A. Fazzio, and A. J. R. da Silva, J. Am. Chem. Soc. **128**, 8996 (2006).
[18] X. D. Cui, A. Primak, X. Zarate, J. Tomfohr, O. F. Sankey, A. L. Moore, T. A. Moore, D. Gust, G. Harris, and S. M. Lindsay, Science **294**, 571 (2001).
[19] H. Akkerman, A. Kronemeijer, P. van Hal, D. de Leeuw, P. Blom, and B. de Boer, Small **4**, 100 (2008).
[20] W. Haiss, S. Martin, L. Scullion, L. Bouffier, S. Higgins, and R. Nichols, Phys. Chem. Chem. Phys. **11**, 10831 (2009).
[21] R. P. Andres, T. Bein, M. Dorogi, S. Feng, J. I. Henderson, C. P. Kubiak, W. Mahoney, R. G. Osifchin, and R. Reifenberger, Science **272**, 1323 (1996).
[22] G. Meshulam, N. Rosenberg, A. Caster, L. Burstein, M. Gozin, and S. Richter, Small **1**, 848 (2005).
[23] L. E. Harrell, T. P. Bigioni, W. G. Cullen, R. L. Whetten, and P. N. First, J. Vac. Sci. Technol. B **17**, 2411 (1999).
[24] T. Ohgi, H. Y. Sheng, and H. Nejoh, Appl. Surf. Sci. **130-132**, 919 (1998).
[25] T. Ohgi, H. Y. Sheng, Z. C. Dong, H. Nejoh, and D. Fujita, Appl. Phys. Lett. **79**, 2453 (2001).
[26] K. Bandyopadhyay and K. Vijayamohanan, Langmuir **14**, 6924 (1998).
[27] N. Vandamme, J. Snauwaert, E. Janssens, E. Vandeweert, P. Lievens, and C. V. Haesendonck, Surf. Sci. **558**, 57 (2004).
[28] T. Nakanishi, B. Ohtani, K. Shimazu, and K. Uosaki, Chem. Phys. Lett. **278**, 233 (1997).
[29] H. Noda, Y. Tai, A. Shaporenko, M. Grunze, and M. Zharnikov, J. Phys. Chem. B **109**, 22371 (2005).
[30] D. Qu and K. Uosaki, J. Phys. Chem. B **110**, 17570 (2006).
[31] T. Nakamura, H. Kondoh, M. Matsumoto, and H. Nozoye, Langmuir **12**, 5977 (1996).
[32] M. Carot, M. Esplandiu, F. Cometto, E. Patrito, and V. Macagno, J. Electroanal. Chem. **579**, 13 (2005).
[33] T. Y. B. Leung, M. C. Gerstenberg, D. J. Lavrich, G. Scoles, F. Schreiber, and G. E. Poirier, Langmuir **16**, 549 (2000).
[34] K. Kobayashi, J. Umemura, T. Horiuchi, H. Yamada, and K. Matsushige, Jpn. J. Appl. Phys., Part 1 **37**, L297 (1998).
[35] K. Kobayashi, H. Yamada, T. Horiuchi, and K. Matsushige, Appl. Surf. Sci. **144-145**, 435 (1999).
[36] J.-J. Yu, J. N. Ngunjiri, A. T. Kelley, and J. C. Garno, Langmuir **24**, 11661 (2008).
[37] M. Esplandiu, M. Carot, F. Cometto, V. Macagno, and E. Patrito, Surf. Sci. **600**, 155 (2006).
[38] J. Liang, L. G. Rosa, and G. Scoles, J. Phys. Chem. C **111**, 17275 (2007).
[39] S. W. Joo, S. W. Han, and K. Kim, J. Phys. Chem. B **104**, 6218 (2000).
[40] P. Kohli, K. K. Taylor, J. J. Harris, and G. J. Blanchard, J. Am. Chem. Soc. **120**, 11962 (1998).
[41] S. Rifai, M. Laferriere, D. Qu, D. D. M. Wayner, C. P. Wilde, and M. Morin, J. Electroanal. Chem. **531**, 111 (2002).
[42] H. Hamoudi, Z. Guo, M. Prato, C. Dablemont, W. Q. Zheng, B. Bourguignon, M. Canepa, and V. A. Esaulov, Phys. Chem. Chem. Phys. **10**, 6836 (2008).
[43] C. D. Bain, E. B. Troughton, Y. T. Tao, J. Evall, G. M. Whitesides, and R. G. Nuzzo, J. Am. Chem. Soc. **111**, 321 (1989).
[44] S. W. Joo, S. W. Han, and K. Kim, Langmuir **16**, 5391 (2000).
[45] J. M. Tour, L. Jones, D. L. Pearson, J. J. S. Lamba, T. P. Burgin, G. M. Whitesides, D. L. Allara, A. N. Parikh, and S. V. Atre, J. Am. Chem. Soc. **117**, 9529 (1995).
[46] K. Suto and O. M. Magnussen (private communication).
[47] M. A. Schneeweiss, H. Hagenström, M. J. Esplandiu, and D. M. Kolb, Appl. Phys. A: Mater. Sci. Process. **69**, 537 (1999).
[48] H. Striegler, P. Skoluda, and D. M. Kolb, J. Electroanal. Chem. **471**, 9 (1999).
[49] S. J. Stranick, M. M. Kamna, and P. S. Weiss, Science **266**, 99 (1994).
[50] J. S. Raut and K. A. Fichthorn, J. Chem. Phys. **108**, 1626 (1998).
[51] J. Weckesser, J. V. Barth, and K. Kern, J. Chem. Phys. **110**, 5351 (1999).
[52] J. V. Barth, Surf. Sci. Rep. **40**, 75 (2000).
[53] J. Weckesser, J. V. Barth, and K. Kern, Phys. Rev. B **64**, 161403(R) (2001).
[54] M. Schunack, T. R. Linderoth, F. Rosei, E. Lægsgaard, I. Stensgaard, and F. Besenbacher, Phys. Rev. Lett. **88**, 156102 (2002).
[55] R. Otero, F. Hümmelink, F. Sato, S. B. Legoas, P. Thostrup, E. Laegsgaard, I. Stensgaard, D. S. Galvao, and F. Besenbacher, Nature Mater. **3**, 779 (2004).
[56] K.-Y. Kwon, K. L. Wong, G. Pawin, L. Bartels, S. Stolbov, and T. S. Rahman, Phys. Rev. Lett. **95**, 166101 (2005).
[57] S. Subramanian and J.-C. Wang, J. Chem. Phys. **123**, 014706 (2005).
[58] J. V. Barth, Annu. Rev. Phys. Chem. **58**, 375 (2007).
[59] G. Pawin, K. L. Wong, K.-Y. Kwon, R. J. Frisbee, T. S. Rahman, and L. Bartels, J. Am. Chem. Soc. **130**, 15244 (2008).
[60] P. Maksymovych, D. C. Sorescu, and J. T. Yates, J. Phys. Chem. B **110**, 21161 (2006).
[61] A. Franke and E. Pehlke, Phys. Rev. B **79**, 235441 (2009).
[62] D. Jiang and S. Dai, J. Phys. Chem. C **113**, 3763 (2009).
[63] D. Jiang and S. Dai, Phys. Chem. Chem. Phys. **11**, 8601 (2009).
[64] G. Kresse and J. Hafner, Phys. Rev. B **47**, 558 (1993).
[65] G. Kresse and J. Hafner, Phys. Rev. B **49**, 14251 (1994).
[66] G. Kresse and J. Furthmüller, Comput. Mater. Sci. **6**, 15 (1996).
[67] G. Kresse and J. Furthmüller, Phys. Rev. B **54**, 11169 (1996).
[68] J. P. Perdew, J. A. Chevary, S. H. Vosko, K. A. Jackson, M. R. Pederson, D. J. Singh, and C. Fiolhais, Phys. Rev. B **46**, 6671 (1992).
[69] P. E. Blöchl, Phys. Rev. B **50**, 17953 (1994).
[70] G. Kresse and D. Joubert, Phys. Rev. B **59**, 1758 (1999).
[71] H. J. Monkhorst and J. D. Pack, Phys. Rev. B **13**, 5188 (1976).
[72] M. Fuchs, M. Bockstedte, E. Pehlke, and M. Scheffler, Phys. Rev. B **57**, 2134 (1998).
[73] H. Shi and C. Stampfl, Phys. Rev. B **77**, 094127 (2008).
[74] P4VASP source code available under http://cms.mpi.univie.ac.at/odubay/p4vasp_site/news.php
[75] J. Tersoff and D. R. Hamann, Phys. Rev. B **31**, 805 (1985).

[76] A. Tkatchenko and M. Scheffler, Phys. Rev. Lett. **102**, 073005 (2009).
[77] S. Grimme, J. Comput. Chem. **27**, 1787 (2006).
[78] F. Ortmann, F. Bechstedt, and W. G. Schmidt, Phys. Rev. B **73**, 205101 (2006).
[79] M. Dion, H. Rydberg, E. Schröder, D. C. Langreth, and B. I. Lundqvist, Phys. Rev. Lett. **92**, 246401 (2004).
[80] *CRC Handbook of Chemistry and Physics*, 76th ed., edited by D. R. Lide (CRC Press, Boca Raton, FL, 1995).
[81] R. Rowland and R. Taylor, J. Phys. Chem. **100**, 7384 (1996).
[82] A. Bondi, J. Phys. Chem. **68**, 441 (1964).
[83] E. McNellis, J. Meyer, and K. Reuter, Phys. Rev. B **80**, 205414 (2009).
[84] C. Vericat, M. E. Vela, G. A. Benitez, J. A. M. Gago, X. Torrelles, and R. C. Salvarezza, J. Phys.: Condens. Matter **18**, R867 (2006).
[85] I. I. Rzeznicka, J. Lee, P. Maksymovych, and J. T. Yates, J. Phys. Chem. B **109**, 15992 (2005).
[86] J.-G. Zhou and F. Hagelberg, Phys. Rev. Lett. **97**, 045505 (2006).
[87] P. Maksymovych, D. C. Sorescu, D. Dougherty, and J. T. Yates, J. Phys. Chem. B **109**, 22463 (2005).
[88] D. J. Lavrich, S. M. Wetterer, S. L. Bernasek, and G. Scoles, J. Phys. Chem. B **102**, 3456 (1998).
[89] H. Grönbeck, A. Curioni, and W. Andreoni, J. Am. Chem. Soc. **122**, 3839 (2000).
[90] M. C. Vargas, P. Giannozzi, A. Selloni, and G. Scoles, J. Phys. Chem. B **105**, 9509 (2001).
[91] Y. Yourdshahyan, H. K. Zhang, and A. M. Rappe, Phys. Rev. B **63**, 081405(R) (2001).
[92] T. Hayashi, Y. Morikawa, and H. Nozoye, J. Chem. Phys. **114**, 7615 (2001).
[93] J. Gottschalck and B. Hammer, J. Chem. Phys. **116**, 784 (2002).
[94] Y. Yourdshahyan and A. M. Rappe, J. Chem. Phys. **117**, 825 (2002).
[95] Y. Cao, Q. Ge, D. J. Dyer, and L. Wang, J. Phys. Chem. B **107**, 3803 (2003).
[96] F. P. Cometto, P. Paredes-Olivera, V. A. Macagno, and E. M. Patrito, J. Phys. Chem. B **109**, 21737 (2005).
[97] N. Gonzalez, N. Lorente, and A. Arnau, Surf. Sci. **600**, 4039 (2006).
[98] R. Mazzarello, A. Cossaro, A. Verdini, R. Rousseau, L. Casalis, M. F. Danisman, L. Floreano, S. Scandolo, A. Morgante, and G. Scoles, Phys. Rev. Lett. **98**, 016102 (2007).
[99] J. Wang and A. Selloni, J. Phys. Chem. C **111**, 12149 (2007).
[100] A. Nagoya and Y. Morikawa, J. Phys.: Condens. Matter **19**, 365245 (2007).
[101] P. Maksymovych, D. C. Sorescu, and J. T. Yates, Phys. Rev. Lett. **97**, 146103 (2006).
[102] Y. Wang, N. S. Hush, and J. R. Reimers, J. Am. Chem. Soc. **129**, 14532 (2007).
[103] Y. Wang, N. S. Hush, and J. R. Reimers, Phys. Rev. B **75**, 233416 (2007).
[104] C. Masens, M. J. Ford, and M. B. Cortie, Surf. Sci. **580**, 19 (2005).
[105] A. Franke and E. Pehlke (unpublished).
[106] D. M. Ceperley and B. J. Alder, Phys. Rev. Lett. **45**, 566 (1980).
[107] J. P. Perdew and A. Zunger, Phys. Rev. B **23**, 5048 (1981).
[108] Polarizabilities in a.u.: $\alpha_{Au}=40$, $\alpha_S=19.6$, $\alpha_C=11.9$, $\alpha_H=4.5$ and first ionization energies in a.u.: $I_{Au}=0.34$, $I_S=0.38$, $I_C=0.41$, $I_H=0.5$.
[109] vdW radii: $R_{Au}=1.66$ Å, $R_S=1.80$ Å, $R_C=1.70$ Å, $R_H=1.09$ Å.
[110] The compressed Au(111)(1×1) model surface is calculated in a rectangular $(4\times2\sqrt{3})$ surface unit cell using a plane-wave cutoff energy of 340 eV, 16 special **k** points in the complete first Brillouin zone, and a slab comprising four Au layers.